TNF-α Impairs the S-G2/M Cell Cycle Checkpoint and Cyclobutane Pyrimidine Dimer Repair in Premalignant Skin Cells: Role of the PI3K–Akt Pathway

Annesofie Faurschou[1], Robert Gniadecki[1], Damien Calay[1,2] and Hans Christian Wulf[1]

Tumor necrosis factor-α (TNF-α) is induced by UVB radiation and has been implicated in the early stages of skin carcinogenesis. Here, we show that in normal keratinocytes and the transformed keratinocyte cell lines, HaCaT and A431, TNF-α stimulates protein kinase B/Akt, which results in activation of the survival complex mTORC1 (mammalian target of rapamycin complex 1) and inhibition of the proapoptotic proteins Bad and FoxO3a. In UVB-irradiated HaCaT cells (10–20 mJ cm^{-2}), TNF-α increased the proportion of cycling cells and enhanced the rate of apoptosis. A significantly higher proportion of UVB-treated HaCaT cells containing unrepaired cyclobutane pyrimidine dimers (CPDs) escaped the G2/M cell cycle checkpoint in the presence of TNF-α (9.5 ± 3.3 vs 4.8 ± 2.2%). After treatment with the PI3K inhibitor LY294002, only 1.2 ± 0.7% of CPD-containing HaCaT cells were actively cycling. TNF-α enhanced apoptosis less potently and did not increase the level of CPD or stimulate cell cycle progression in normal keratinocytes. Our data suggest that TNF-α overrides the G2/M checkpoint in premalignant skin cells and allows for some cells containing unrepaired CPD to enter the cell cycle. The effect of TNF-α seems to be dependent on Akt activation and may constitute a relevant mechanism enhancing mutagenesis and tumor development.

Journal of Investigative Dermatology (2008) **128,** 2069–2077; doi:10.1038/jid.2008.19; published online 14 February 2008

INTRODUCTION

Besides its well-known role in inflammation, tumor necrosis factor-α (TNF-α) is involved in skin carcinogenesis. TNF-α- and the TNF type 1 receptor knockout mice are protected against squamous cell carcinoma (Moore *et al.*, 1999; Arnott *et al.*, 2004). In keratinocytes, TNF-α signals predominantly via the TNF type 1 receptor and the TRADD–TRAF2–RIP complex, which causes activation of the atypical protein kinase C species (PKCζ, PKCλ/ι) and the transcription factor NF-κB (Anthonsen *et al.*, 2001; Lisby *et al.*, 2006). Whereas in normal keratinocytes NF-κB signaling seem to protect against squamous cell carcinoma, deregulated NF-κB activity in initiated tumor cells confers the antiapoptotic, mitogenic signal (Dajee *et al.*, 2003; Loercher *et al.*, 2004). In immortalized, nontumorigenic HaCaT keratinocytes, which serve as a model of an early, transformed epidermal cancer cell, TNF-α-induces NF-κB and inhibits anoikis (Ren *et al.*, 2006). Among many possible mechanisms, NF-κB inhibits the tumor suppressor gene PTEN (phosphatase and tensin homologue deleted from chromosome 10) (Kim *et al.*, 2004; Vasudevan *et al.*, 2004), the most potent repressor of Akt kinase signaling pathway. Earlier studies indicate that TNF-α is able to activate Akt (Ozes *et al.*, 1999), but this has not been seen in all cell types (Janes *et al.*, 2006).

A previous study indicates that TNF-α is able to modulate the activity of Akt in keratinocytes (Zhang *et al.*, 2001). This question is relevant, as hyperactivation of Akt is an important step facilitating tumor development and progression in a majority of cancers (Altomare and Testa, 2005). Disturbances in Akt-signaling pathway have recently been demonstrated in human and murine squamous cell carcinoma (Suzuki *et al.*, 2003; Segrelles *et al.*, 2006). Mice with hyperactivated Akt due to keratinocyte-specific PTEN knockout show hyperplastic and hyperkeratotic epidermis and display elevated sensitivity to chemical carcinogens and spontaneous development of papillomas and carcinomas (Suzuki *et al.*, 2003).

We provide evidence that, in normal keratinocytes and in the immortalized cell line HaCaT (a model of the precancerous skin lesion (Ren *et al.*, 2006)) and the human squamous cell carcinoma cell line A431, TNF-α upregulates the activity of Akt, which results in the activation of its downstream effector molecular target mTORC1 and inhibition of the proapoptotic proteins Bad and FoxO3a. We show that TNF-α

[1]*Department of Dermatology, University of Copenhagen, Bispebjerg Hospital, Copenhagen, Denmark and* [2]*Department of Histology-Embryology, Faculty of Medicine, University of Namur, Namur, Belgium*

Correspondence: Dr Annesofie Faurschou, Department of Dermatology D, Bispebjerg Hospital, Bispebjerg Bakke 23, Copenhagen DK-2400, Denmark. E-mail: Af16@bbh.regionh.dk

Abbreviations: BrdU, bromodeoxyuridine; CPD, cyclobutane pyrimidine dimmer; LSC, laser scanning cytometry; NAC, N-acetylcysteine; NHK, normal human keratinocyte; PBS, phosphate-buffered saline; PI, propidium iodide; TNF-α, tumor necrosis factor-α

Received 2 February 2007; revised 21 November 2007; accepted 19 December 2007; published online 14 February 2008

impairs repair of UVB-induced cyclobutane pyrimidine dimers (CPDs) in HaCaT cells via an Akt-dependent pathway.

RESULTS

TNF-α induces Akt and its downstream effector pathways (mTORC1, Bad, and FoxO3a) in normal human keratinocytes and HaCaT cells

Our previous research determined that in cultured murine and human keratinocytes and in HaCaT cells, TNF-α activates NF-κB and the transcription of its own gene in the concentration range of 10–50 ng ml^{-1} via the TNF type 1 receptor (Lisby *et al.*, 2006). Treatment with 10 ng ml^{-1} recombinant human TNF-α resulted in double phosphorylation of Ser-473 and Thr-308 in Akt, reflecting its enzymatic activation (Figure 1). PI3K inhibitors, LY294002 (Figure 1) and wortmannin (not shown), blocked the TNF-α-induced activation of Akt in HaCaT cells. Similarly, LY294002 and wortmannin have been described to inhibit Akt phosphorylation in normal human keratinocytes (NHKs) (Wang *et al.*, 2003). To investigate the physiological consequences of the TNF-α-induced phosphorylation of Akt, we examined the functional status of its three main targets: the transcription factor FoxO3a, the proapoptotic protein Bad, and the survival complex mTORC1. Akt regulates FoxO3a via complex, multiple phosphorylations, which cause the deactivation and translocation of FoxO3a from the nucleus to the cytoplasm (Biggs III *et al.*, 1999). As shown in Figure 1c, FoxO3a became rapidly translocated from the nucleus to the cytoplasm upon treatment with TNF-α. This effect could be inhibited by LY2944002. Another important downstream pathway activated by Akt is the rapamycin-sensitive mTOR complex 1 (mTORC1)-p70^{S6K} via the tuberous sclerosis proteins TSC1 and TSC2 and small GTPase Rheb (Wullschleger *et al.*, 2006). Figure 1a–b documents that the treatment with TNF-α resulted in phosphorylation of p70^{S6K} confirming the activation of mTORC1 by this cytokine. Finally, we also observed that Bad became rapidly phosphorylated on Ser^{112} by TNF-α (Figure 1b), which has previously been shown to mediate binding to 14-3-3 proteins and Bad inactivation (Zha *et al.*, 1996). Taken together, these data provided evidence that TNF-α caused a functional activation of Akt in keratinocytes.

TNF-α augments Akt phosphorylation in UVB-irradiated keratinocytes

As the purpose of this study was to investigate how TNF-α modulates the physiologic response of the keratinocytes to UV radiation, we determined whether this cytokine also induced Akt activity in UVB-irradiated HaCaT cells. In accordance with previous data (Wang *et al.*, 2003), we showed that UVB induced Akt activity in HaCaT (Figure 2), A431, and normal keratinocytes (not shown). Relevant doses

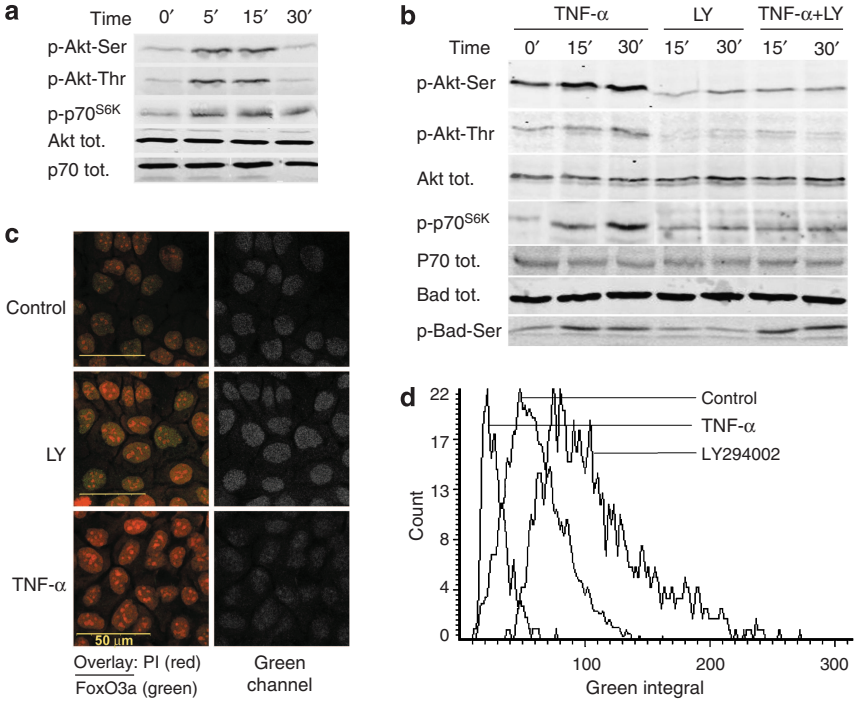

Figure 1. TNF-α induces Akt via the PI3K-sensitive pathways. Cultured cells ((**a**) NHKs; (**b–d**) HaCaT) were treated with 10 ng ml^{-1} TNF-α for 0–30 minutes with or without the PI3K blocker, LY294002 (20 μM). Protein extracts were analyzed with western blotting using antibodies against phosphorylated Akt (Ser473; Thr308); total Akt, phosphorylated p70^{S6K} or total and phosphorylated Bad (Ser112) at the indicated times of incubation with TNF-α. (**c**, **d**) Inactivation of FoxO3a by TNF-α in HaCaT cells. Cells were treated with 20 μM LY294002, 10 ng ml^{-1} TNF-α or the vehicle (control) for 3 or 24 hours and stained with the mAb against FoxO3a. Nuclear DNA was labeled with PI/RNase solution. The cells were imaged by (**c**) confocal microscopy (3 hours) or (**d**) scanned by LSC (3 hours; green-FoxO3a, red-PI) to determine integral nuclear FoxO3a fluorescence. Bar = 50 μm. The histograms represent $n = 5{,}000$ cells.

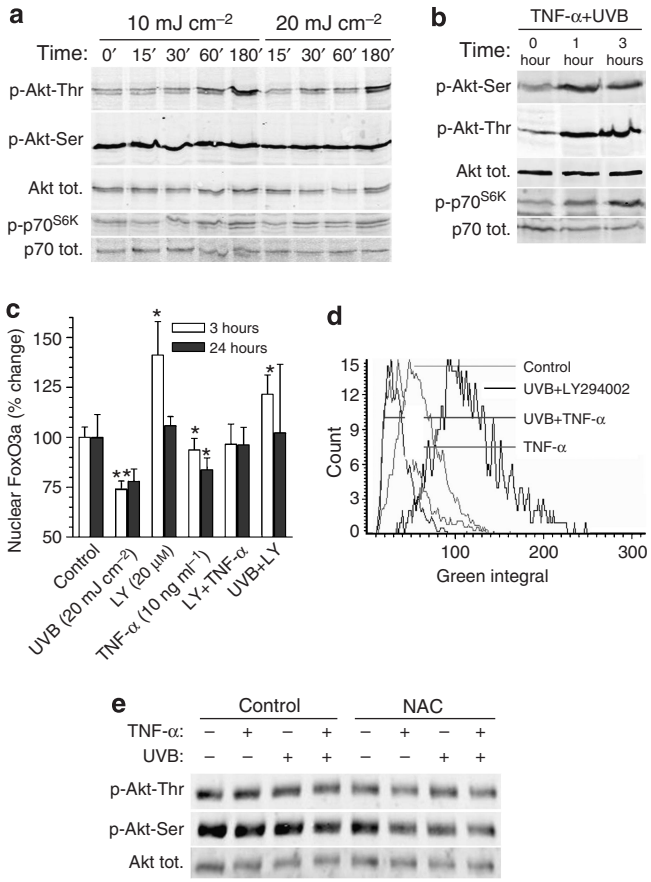

Figure 2. TNF-α induces Akt in UVB-irradiated cells. Cultured HaCaT cells were irradiated with 10 or 20 mJ cm^{-2} UVB, alone or in combination with 10 ng ml^{-1} TNF-α. (**a**, **b**) Protein extracts were analyzed with western blotting as shown in Figure 1. (**c**, **d**) Inactivation of FoxO3a by UVB and TNF-α in HaCaT cells. UVB-irradiated (20 mJ cm^{-2}) and non-irradiated cells were treated with 20 μM LY294002, 10 ng ml^{-1} TNF-α, or the vehicle (control) for 3 or 24 hours and FoxO3a and DNA were stained as shown in Figure 1. (**c**) Average nuclear fluorescence intensity calculated by image analysis of 10–20 cells from confocal images, $*P<0.05$, *t*-test in comparison to the vehicle-treated non-irradiated control. (**d**) Integral nuclear FoxO3a fluorescence ($n=5{,}000$ cells) obtained by LSC 3 hours after irradiation as shown in Figure 1. (**e**) Cultured cells, HaCaT, were treated with NAC for 45 minutes, irradiated with 20 mJ cm^{-2} UVB, and/or treated with 10 ng ml^{-1} TNF-α for 15 minutes. Protein extracts were analyzed with western blotting as in Figure 1.

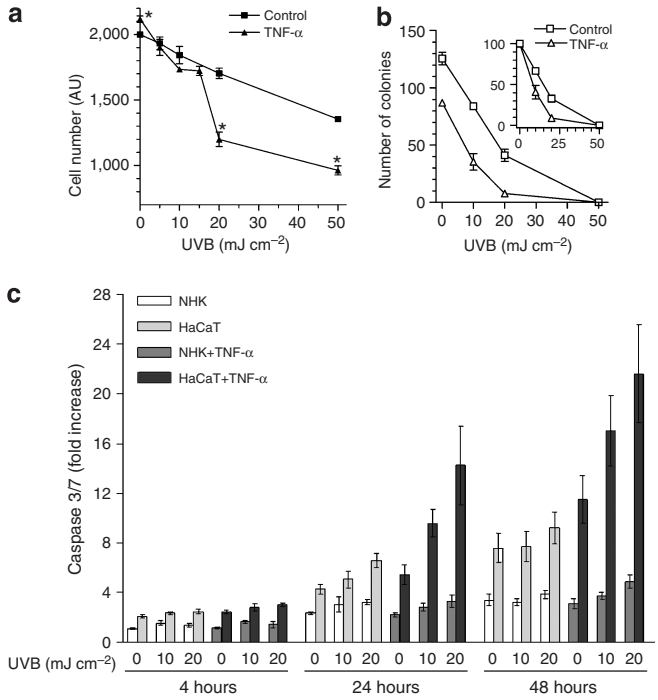

Figure 3. Apoptosis of UVB-irradiated cells in the presence of TNF-α. (**a**) Cultured HaCaT cells were irradiated with 0–50 mJ cm^{-2} UVB and cultured in the absence or presence of TNF-α for 24 hours. Cell survival was determined by a (**a**) methylene blue assay or (**b**) clonogenic assay. Inset graph in (**b**) shows the same data expressed as the % of control baseline. $n=3$, bars: SD. (**c**) The level of apoptosis was determined by the caspase 3 and 7 activity 4, 24, and 48 hours after irradiation with 0, 10, and 20 mJ cm^{-2} UVB for NHKs and HaCaT cells cultured in the presence of TNF-α. The shown values are means of $n=4$ experiments with SD.

of UVB (10–20 mJ cm^{-2}) caused a moderate increase in Akt phosphorylation especially on the Thr^{308} residue, 2.8-fold increase in phosphorylation of p70^{S6K} (20 mJ cm^{-2}, 180 minutes), and deactivation of FoxO3a and Bad in HaCaT cells (Figure 2). This effect was partially dependent on reactive oxygen species, as the superoxide scavenger *N*-acetylcysteine (NAC) reduced UVB-dependent Akt phosphorylation (Figure 2f). α-Tocopherol, a singlet oxygen-quenching agent did not affect UV-induced Akt/p70 activation, suggesting the primary involvement of the superoxide (data not shown). When UVB irradiation was administered to the TNF-α-treated HaCaT cells, the Akt phosphorylation was more pronounced on both phosphorylation sites, the effect of which was reduced by the concomitant administration of NAC (Figure 2b, c and f) but not α-tocopherol (not shown).

Inhibition of PI3K–Akt signaling by LY294002 blocks the TNF-α-dependent S-phase entry and cell cycle progression in HaCaT cells

The Akt-signaling pathway confers the antiapoptotic, pro-survival signals, which in many cell types result in increased S-phase entry, accelerated cell growth, and resistance to death signals (Sun *et al.*, 1999). Clonogenic growth of HaCaT cells cultured in the presence of 10–100 ng ml^{-1} TNF-α did not differ from those of vehicle-treated cells (not shown). This excludes any major cytotoxic effect or long-term modulation of cell growth. However, in a 24 hours growth assay, TNF-α had a small, but significantly growth-enhancing, effect (Figure 3a). This was further confirmed by the bromodeoxyuridine (BrdU) incorporation assay where TNF-α-treated HaCaT cells showed a higher proportion of S-phase-labeled cells and shorter S-G1 transition time. As could be expected, LY294002 retarded cell cycle, causing a G0/G1 arrest at 24 hours (Figure 4a). LY294002 abrogated also the stimulatory effects of TNF-α on DNA synthesis (Figure 4a). Thus, inhibition of the PI3K–Akt axis rendered the cells mitotically unresponsive to TNF-α, indicating that this signaling pathway was responsible for the mitogenic effect of this cytokine.

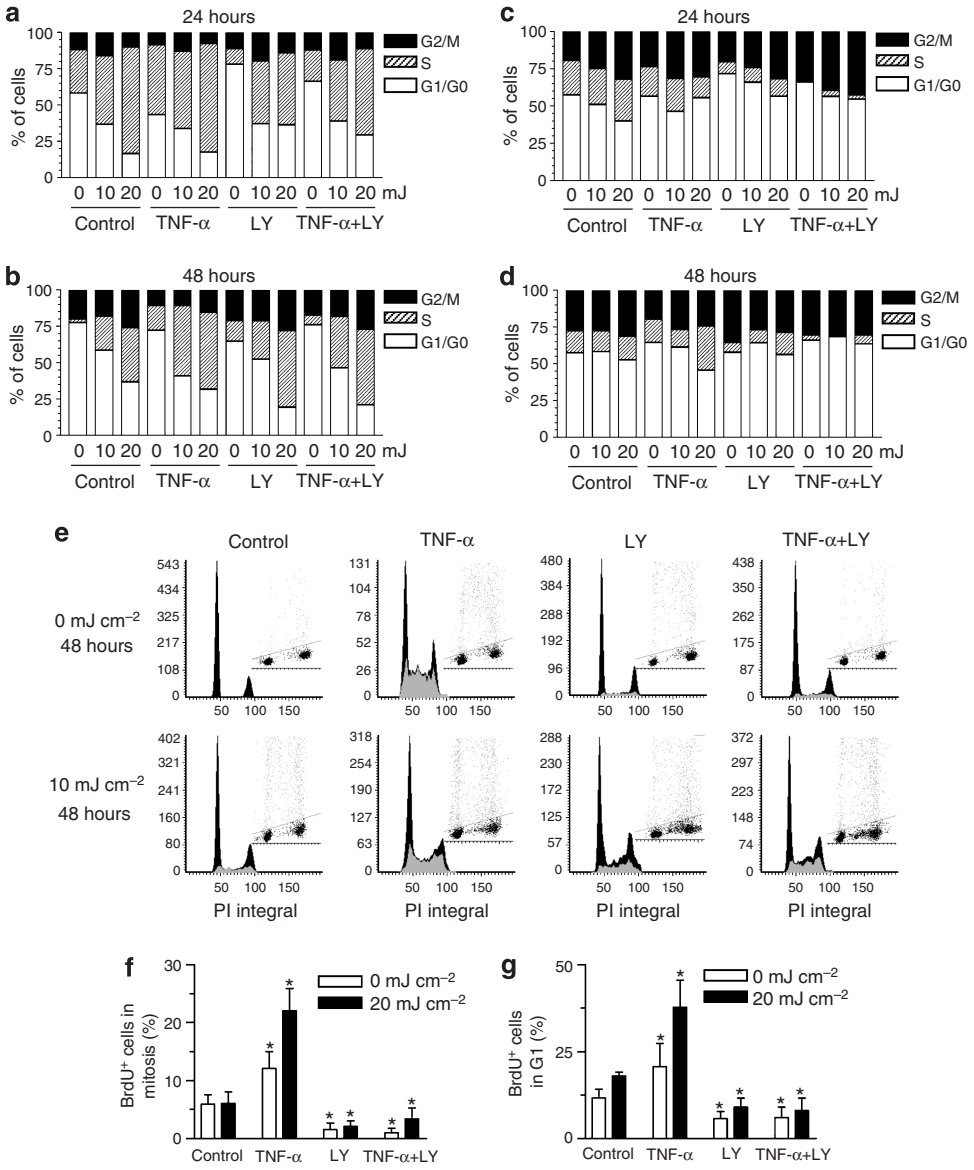

Figure 4. TNF-α stimulates S-phase entry and overrides G2 block in UVB-irradiated cells. (**a**) Cultured HaCaT cells and (**b**) NHKs were irradiated with 0–20 mJ−cm^{-2} UVB and cultured for 24–48 hours in the presence of TNF-α, LY294002 or the vehicle (control), as indicated. Cells were pulse-labeled with 10 μM BrdU, fixed and stained with anti-BrdU antibody and PI/RNase, and analyzed by LSC to determine the proportion of cells in different phases of cell cycle. Proportion of (**a**, **b**) HaCaT cells and (**c**, **d**) NHKs in G0/G1, S, and G2/M phases in experimental groups calculated from cell-cycle histograms. (**e**) Cells were pulse-labeled 30 minutes before the termination of the experiment, and DNA histograms with corresponding dot-plots showing BrdU-positive S-phase cells (gray) were created. *x* axis on histograms and dot plots represents total (integrated) nuclear PI fluorescence. (**f**) Cells were pulse-labeled with BrdU for 30 minutes and chased for 2 hours in the presence of colcemid. The number of labeled mitoses was calculated manually from four viewfields in microscopic epifluorescent images. Means ($n=3$) with SD. (**g**) Cells were pulse-labeled with BrdU for 30 minutes, chased for 3 hours, fixed, stained and LSC-scanned as in (**c**). The number of labeled cells in G1 phase is shown in relation to the total number of G1 cells. Means ($n=3$) with SD.

TNF-α decreases efficacy of S-G2 cell cycle block in UVB-irradiated HaCaT cells via a PI3K–Akt-dependent pathway

HaCaT cells have a defective G1 cell cycle checkpoint and respond to DNA damaging stimuli by arrest in S and G2 phases (Thorn *et al.*, 2001). An intensity of 10–20 mJ cm^{-2} UVB caused a dose-dependent decrease in G1 phase cells and increase in S and G2 cells, both 24 and 48 hours after irradiation in HaCaT cells and normal keratinocytes (Figure 4). In comparison to the control cells, TNF-α caused a marked increase in the proportion of actively cycling, BrdU-incorporating HaCaT cells in S-phase and decreased the proportion of G2/M cells after UVB irradiation. Pulse-chase experiments revealed a more rapid cell-cycle transition of TNF-α-treated UVB-irradiated HaCaT cells, which could be reversed by treatment with LY294002 (Figure 4). In normal keratinocytes, TNF-α did not stimulate DNA synthesis and cell cycle progression, but acted synergistically with LY294002, reducing the amount of S phase cells and

retarding the cell cycle (Figure 4). In conclusion, TNF-α seemed to increase the transition through the cell cycle and attenuated the S-G2 block imposed by UVB in HaCaT cells.

TNF-α enhances survival and proliferation of HaCaT cells containing unrepaired CPD lesions

As G2 cell cycle checkpoint is relieved when DNA lesions are repaired, we asked whether the attenuation of G2 cell cycle block was caused by an enhanced DNA repair of TNF-α-treated HaCaT cells. As shown in Figure 5a, the TNF-α-treated cells exhibited a significantly higher level of CPD than the control cells, both 24 and 48 hours after UVB irradiation. The cell death assays (methylene blue absorption test and clonogenic assay) as well as the apoptosis-specific caspase 3/7 activity assay revealed increased apoptotic levels after TNF-α treatment (Figure 3). NAC did not affect the CPD levels in the UVB-irradiated and TNF-α-treated or control HaCaT cells (not shown). In normal keratinocytes, no significantly elevated levels of CPD was found after irradiation with UVB and treatment with TNF-α compared to controls. Exposure to UVB resulted in significantly less apoptotic cells among normal keratinocytes than HaCaT cells. TNF-α did not enhance cell death of normal keratinocytes at low UVB dose (10 mJ cm^{-2}) but increased apoptosis significantly 48 hours after a high dose of UVB (20 mJ cm^{-2}) (Figure 3). From these experiments, we concluded that increased CPD content in HaCaT cells treated with TNF-α was caused by impaired DNA repair and not impaired removal of irreversibly damaged cells.

CPD-containing HaCaT cells could be detected by laser scanning cytometry (LSC) or confocal microscopy after staining with the specific antibody. The CPD^{bright} cells were distributed in all phases of cell cycle and were more numerous

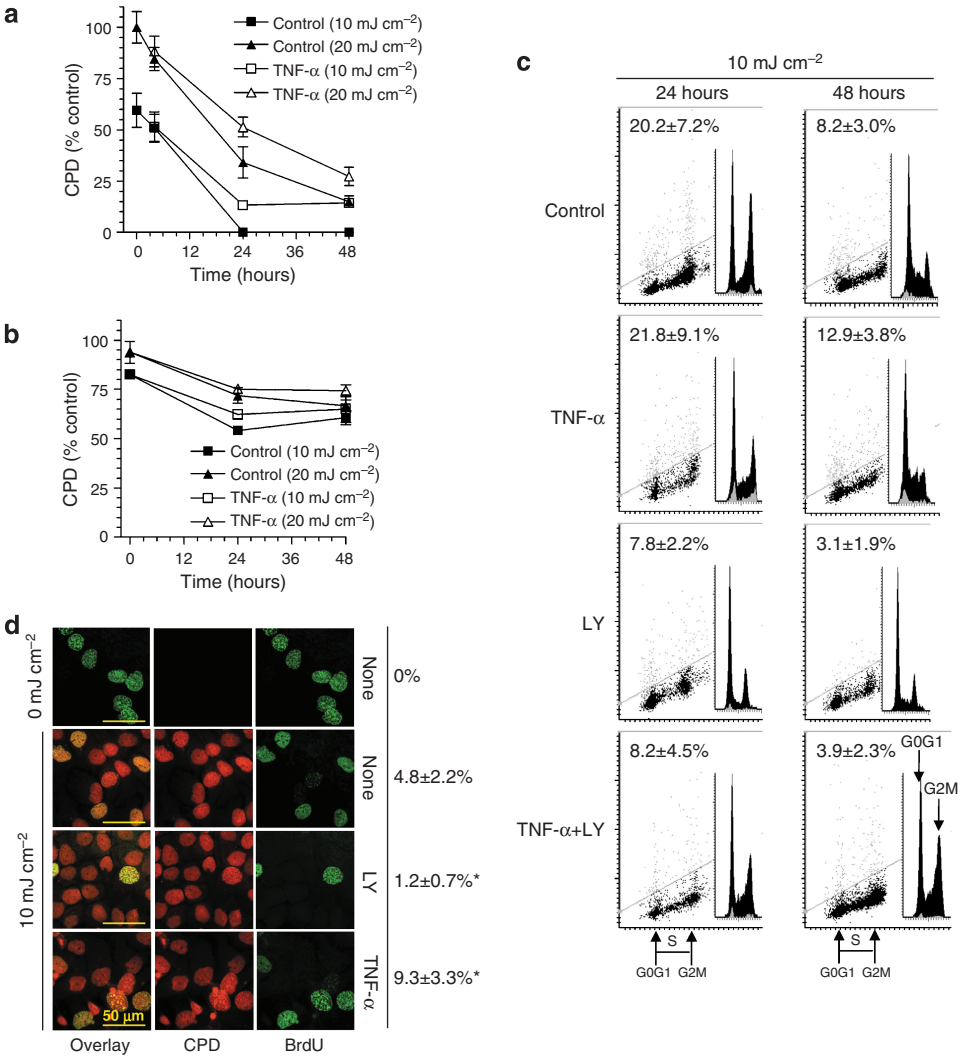

Figure 5. Impaired clearance of UVB-induced CPD lesions in TNF-α-treated HaCaT cells. Cells pretreated for 1 hour with 0 or 10 ng ml^{-1} TNF-α were irradiated with the indicated doses of UVB. The dynamics of DNA repair was determined by ELISA specific for CPD for (**a**) HaCaT cells and (**b**) NHKs. In (**c**), HaCaT cells were doubly labeled with an antibody against CPD and with PI and analysed by LSC. Dot plots represent total nuclear CPD staining plotted against PI. (**d**) Double labeling of cells 24 hours after irradiation with 0 (sham) or 10 mJ cm^{-2} UVB with the anti-CPD antibody (red) and anti-BrdU (green). The cells were treated with LY294002, 10 ng ml^{-1} TNF-α, or left untreated (control) and pulsed with BrdU 2 hours before the termination of the experiment. The numbers show percentage of BrdU + CPD^{bright} cells (means $n = 20$ with SD). Bar = 50 µm.

in the TNF-α-treated cells, confirming the data gathered by CPD ELISA (Figure 5). To establish whether the CPD^{bright} cells were mitotically active, we pulse-labeled the cultures with BrdU and stained them with the specific antibody against CPD. In this experiment, we observed that the cells containing relatively high levels of nuclear CPD were able to enter S phase and later mitosis (Figure 5c). The proportion of these cells was significantly higher in the TNF-α-treated cultures ($P<0.003$). This effect of TNF-α could be counteracted by LY294002, which restored the G2 cell cycle block and caused a general decrease in the number of CPD^{bright} cells.

DISCUSSION

UVB radiation is directly absorbed by DNA and causes formation of mutagenic CPDs. Although most CPDs are removed by nucleotide excision repair mechanisms, at least two other protective mechanisms exist in the cells to minimize the risk of mutations: the cell cycle checkpoints that enable cell cycle arrest and provide more time for DNA repair, and apoptosis by which cells containing elevated levels of CPD are permanently removed. The main finding of this study is that TNF-α overrides the cell cycle checkpoints and modulates the apoptotic response to UVB in premalignant skin cells. The net result is an increased number of mitotically active cells with unrepaired DNA.

TNF-α is secreted after irradiation with UVB in normal epidermis and in cultured NHKs and HaCaT cells (Kock *et al.*, 1990). Earlier studies documented the role of this cytokine as an accelerator of UVB-induced apoptosis (Schwarz *et al.*, 1995). Here, we confirm that TNF-α enhances cell death after UVB. TNF-α also affects the cell cycle. Although long-term exposure to TNF-α did not increase the cell number in a 2-week clonogenic assay, a short-term treatment increased acutely the proportion of mitotically active HaCaT cells (measured by the number of S-phase cells). The increase in S-phase in TNF-α-treated HaCaT cells was not due to the G2/M delay, as the proportion of G2/M cells was not different from the control, and the S-G1 transition time measured as a proportion of BrdU-labeled cells that reappeared in G1 after 2 hours in a pulse-chase experiment was increased after TNF-α treatment.

Protein kinase B/Akt is a central kinase involved in the regulation of cell cycle progression, DNA damage checkpoint control and apoptosis. Murine models indicate that in normal epidermis the Akt-signaling pathway is responsible for keratinocyte differentiation and survival (Peng *et al.*, 2003; Calautti *et al.*, 2005). Abnormal activation of Akt is found is squamous cell carcinomas and sensitizes keratinocytes to spontaneous and mutagen-induced transformation (Suzuki *et al.*, 2003; Segrelles *et al.*, 2006). Overexpression of Akt stimulates cellular metabolism and enhances mitotic activity by enhancing S-phase entry (Sun *et al.*, 1999). We have hypothesized that TNF-α could exert some of the above-described effects via Akt signaling. Indeed, measurement of Akt phosphorylation status revealed increased $P\text{-}Thr^{308}$ and $P\text{-}Ser^{473}$ in TNF-α-treated NHK, HaCaT, and A431 cells synonymous with Akt activation. HaCaT cells contain high baseline levels of $Akt^{P-Ser473}$, and Akt activity is mainly regulated by the second phosphorylation site on Thr^{308}. The above-described effects of TNF-α on HaCaT cell apoptosis and accelerated S-phase entry were PI3K dependent, as they could be reversed by LY294002 and were thus at least partially mediated by Akt. Other signaling pathways may also be involved. Activation of the mitogen-activated protein kinase 7/c-Jun-NH_2-kinase/activator protein 1 cascade through the TNF type 1 receptor has recently been shown to play an important role in TNF-α-mediated cutaneous carcinogenesis (Zhang *et al.*, 2007). In line with a previous report (Zhang *et al.*, 2001), we could confirm that the superoxide scavenger NAC, but not the singlet oxygen quenching agent α-tocopherol, reduced the TNF- and UVB-induced Akt activation.

We found that TNF-α had a significant impact on cell kinetics and DNA repair after UVB irradiation. TNF-α-treated HaCaT cells showed a less prominent accumulation of cells in the G2/M phase than the UVB-irradiated controls. This was associated with a higher proportion of $BrdU^+$ cycling cells in the TNF-α-treated UVB-irradiated cells, in comparison to the irradiation alone. After UVB irradiation, a significantly higher proportion of TNF-α-treated HaCaT cells containing unrepaired CPD and mitotically active $BrdU^+$ cells. In normal keratinocytes, TNF-α did not increase the level of CPD or stimulate cell cycle progression. One of the reasons for this difference could be the aberration in NF-κB signaling and p53 signaling in HaCaT cells (Boukamp *et al.*, 1995; Ren *et al.*, 2006). Thus, the TNF-α-Akt signaling is likely to play a role at the tumor promotion rather than the initiation stage, a conclusion that has also been reached by other researchers (Altomare and Testa, 2005).

Even though TNF-α eliminates the cells with UV-induced DNA lesions via enhanced apoptosis, this cytokine overrides the G2/M checkpoint in premalignant skin cells and allows for some cells containing unrepaired CPD to enter cell cycle. In other cell types, it has similarly been shown that Akt activation can overcome cell cycle arrest at G1 and G2/M checkpoints induced by DNA damage and that cells continue to divide and accumulate mutations (Henry *et al.*, 2001; Kandel *et al.*, 2002). Our data suggest that the effect of TNF-α is dependent on the activation of Akt and may constitute a relevant mechanism enhancing mutagenesis and tumor development.

TNF-α treatment led to PI3K-dependent activation of the survival complex mTORC1-$p70^{S6K}$ and inactivation of the proapoptotic protein Bad and the transcription factor FoxO3a, the canonical downstream targets of Akt. The activated, dephosphorylated FoxO3a is able to block cell proliferation and induce cell death via bim (Dijkers *et al.*, 2000) and bcl-xL (Tang *et al.*, 2002). Thus, FoxO transcription factors are generally regarded as antiproliferative tumor suppressors (Hu *et al.*, 2004; Greer and Brunet, 2005). In the skin, the Akt-dependent deactivation of FoxO3a contributes to squamous cell carcinoma formation in mice, and probably also in humans (Segrelles *et al.*, 2006). Among several mechanisms explaining the involvement of FoxO3a in carcinogenesis, this factor positively affects DNA repair via p53 and G1/S and G2/M cell cycle arrest (Medema *et al.*,

2000; Ramaswamy *et al.*, 2002; Tran *et al.*, 2002; You *et al.*, 2006). Thus, the TNF-α–Akt–FoxO3a axis may play a role in the observed G2/M checkpoint suppression.

MATERIALS AND METHODS

Cell culture

NHKs were purchased from CELLnTEC Advanced Cells Systems (Bern, Switzerland) and cultured in epidermal keratinocyte medium (CELLnTEC) according to the manufacturer's instructions. HaCaT cells (Boukamp *et al.*, 1988) was provided by Dr M.R. Pittelkow (Mayo Clinic, Rochester, MI) and A431 cells were obtained from the American Type Culture Collection (Manassas, VA). The cells were grown in DMEM and MEM, respectively, supplemented with 10% fetal calf serum at 37°C in a humidified incubator with 5% CO_2. The cell culture reagents were purchased from Gibco BRL (Life Technologies, Rockville, MD). The cells were tested regularly to be negative for *Mycoplasma*.

Reagents and antibodies

LY294002 was from Calbiochem (EMD Biosciences Inc., Darmstadt, Germany); all other chemicals including recombinant human (rhu) TNF-α were from Sigma-Aldrich (St Louis, MO). Antibodies against phosphorylated Akt (Ser473; Thr308), phosphorylated $p70^{S6K}$, total $p70^{S6K}$, phosphorylated Bad (Ser112), and total FoxO3a were purchased from Cell Signaling (Beverly, MA). Anti-CPD antibodies were from MBL International (Woburn, MA), the anti-AKT and the anti-Bad antibodies from BD Transduction Laboratories (BD Biosciences, San Jose, CA). Anti-BrdU was from Abcam (Cambridge, UK). Secondary antibodies were Texas red-labeled goat anti-mouse antibody (Jackson Laboratories, Bar Harbor, ME) or FITC-conjugated polyclonal porcine anti-rabbit or anti-rat antibody (DakoCytomation, Glostrup, Denmark) or Alexa 488-conjugated anti-mouse antibody (Molecular Probes, Invitrogen Corporation, Carlsbad, CA).

UVB irradiation

The cells were irradiated from above in phosphate-buffered saline (PBS) with doses ranging from 0 to 50 mJ cm^{-2} by calibrated Philips TL12 UVB tubes (Philips, Eindhoven, The Netherlands) with a peak output around 313 nm.

Survival assays

HaCaT cells were seeded in 24-well plates at 100,000 cells per well and allowed to adhere overnight. After treatment, the cells were fixed with 4% paraformaldehyde and stained with 0.1% aqueous methylene blue solution for 15 minutes. The dye was extracted with 0.1 M HCl and absorbance was measured at 595 nm (Ultraspec III spectrophotometer, Pharmacia, Uppsala, Sweden). For the clonogenic growth assay, the cells were seeded into 10 cm Petri dishes (500 per dish) and allowed to adhere for 24 hours. The next day, the cells were treated with UVB and incubated with rhu-TNF-α or LY294002 for 24 hours. After 14 days, the colonies were fixed with 2% paraformaldehyde, stained with 1% crystal violet, and counted manually if larger than 2 mm.

Western blot analysis

The cells were seeded in 6 cm Petri dishes and allowed to grow to 80% confluence. Cells were washed twice in PBS and subsequently lysed in 200 μl of sample buffer (0.5 M Tris-HCl, pH 6.8; 5% glycerol; 10% SDS; DTT 0.2 M).

Bio-Rad Protein Assay kit (Bio-Rad Laboratories, Hercules, CA) was used to quantify the protein concentration of each sample according to the manufacturer's instructions. An equal amount of total cellular protein (50–100 μg) was separated by a 10% SDS-PAGE at 150 V before wet electrotransfer onto a nitrocellulose membrane (Bio-Rad Laboratories). Membranes were blocked for 1 hour at 4°C with Li-Cor blocking agent (Lincoln, NE) followed by incubation with either primary mouse or rabbit antibody overnight at 4°C. After the membranes were washed, they were exposed to secondary antibodies labeled with 700IR dye (anti-mouse) or 800IR dye (anti-rabbit) (both obtained from Li-Cor) followed by detection and quantification of the protein bands with the infrared Odyssey imaging System (Li-Cor).

CPD quantification by ELISA

HaCaT cells were seeded in 6 cm Petri dishes at 300,000 per dish and cultured for 1 day before UV irradiation. After treatment, the cells were scraped in 100 μl PBS, suspended in 500 μl lysis buffer, and extracted using Invisorb Spin Cell Mini Kit (Invitek, Berlin, Germany) as described by the manufacturer. DNA concentration and purity was measured using a NanoDrop ND-1000 spectrophotometer (PEQLAB Biotechnologie, Erlangen, Germany).

CPDs were detected by ELISA as recommended by MBL International Corporation (Woburn, MA). Briefly, DNA samples were denatured at 100°C for 10 minutes, chilled rapidly in an ice bath for 15 minutes, and transferred at a concentration of 1 μg ml^{-1} to a flat-bottomed 96-well microtiter plate coated with 0.003% protamine sulfate. The plates were allowed to dry overnight at 37°C. Next morning, the plates were incubated with 2% fetal calf serum in PBS to prevent nonspecific antibody binding before incubation with anti-CPD antibodies. After washing, the plates were incubated with Biotin-$F(ab)_2$ fragment of anti-mouse IgG (H + L) (Invitrogen, Carlsbad, CA) followed by treatment with peroxidase-streptavidin (Invitrogen) and incubation with the *O*-phenylene diamine substrate solution. The absorbance was determined at 492 nm.

Laser scanning cytometry

For BrdU staining, the cells were cultured on coverslips and incubated with BrdU for 30 minutes before termination of the experiment. Subsequently, the cells were fixed at 4°C in 4% paraformaldehyde for 20 minutes, permeabilized with 1% Triton X-100 for 10 minutes, and then rehydrated with 0.5% PBS/BSA for 15 minutes. DNA was denatured with 2 M HCl for 30 minutes followed by staining with rat anti-BrdU antibody for 30 minutes at room temperature and 50 μg ml^{-1} propidium iodide (PI) with 200 μg ml^{-1} RNase in PBS for 10 minutes at 4°C. In some experiments, the cells were treated with 0.1 μg ml^{-1} colcemid. Integrated single-cell fluorescence was measured by LSC (CompuCyte Corp., Cambridge, MA) as described previously (Thorn *et al.*, 2001). The fluorescence was recorded from approximately 5,000 cells and captured using WinCyte software (CompuCyte). For CPD staining, the samples were processed identically to the staining for BrdU, except for the anti-BrdU being replaced with murine anti-CPD antibody (1:2,500). For FoxO3a staining, the cells were fixed and permeabilized as above, but the HCl denaturation step was omitted.

Confocal microscopy

HaCaT cells were seeded on coverslips, stained as for LSC, and imaged by an Olympus IX70 confocal laser scanning microscope (Olympus, FluoView Confocal System). The fluorescence intensity average was determined for approximately 20 cells in each experiment using the proprietary Fluoview software.

Quantification of apoptosis

The Caspase-Glo 3/7 (Promega Corporation, Madison, WI) was used to quantify the UVB-induced cell death after treatment with TNF and LY according to the manufacturer's instructions. Luminescence was measured using a Wallac 1420 Victor3 II microplate-based luminometer (PerkinElmer, Wellesley, MA).

Statistics

Experiments were conducted in duplicate or triplicate and repeated 2–3 times. Data are presented as means with standard deviation (SD). Groups were compared using two-sided *t*-test or ANOVA. Obtaining a *P*-value of less than 0.05 was considered significant. The software used was GraphPad Prism Version 4.03 (GraphPad Software Inc., San Diego, CA) or Excel (Microsoft Corp., Redmond, WA). Institutional approval of the experiments was not necessary.

CONFLICT OF INTEREST

The authors state no conflict of interest.

ACKNOWLEDGMENTS

We thank Ms Ingelise Pedersen, Ms Eva Hoffman, and Mrs Vibeke Pless for excellent technical assistance.

REFERENCES

Altomare DA, Testa JR (2005) Perturbations of the AKT signaling pathway in human cancer. *Oncogene* 24:7455–64

Anthonsen MW, Andersen S, Solhaug A, Johansen B (2001) Atypical lambda/iota PKC conveys 5-lipoxygenase/leukotriene B4-mediated cross-talk between phospholipase A2s regulating NF-kappa B activation in response to tumor necrosis factor-alpha and interleukin-1beta. *J Biol Chem* 276:35344–51

Arnott CH, Scott KA, Moore RJ, Robinson SC, Thompson RG, Balkwill FR (2004) Expression of both TNF-alpha receptor subtypes is essential for optimal skin tumour development. *Oncogene* 23:1902–10

Biggs WH III, Meisenhelder J, Hunter T, Cavenee WK, Arden KC (1999) Protein kinase B/Akt-mediated phosphorylation promotes nuclear exclusion of the winged helix transcription factor FKHR1. *Proc Natl Acad Sci USA* 96:7421–6

Boukamp P, Petrussevska RT, Breitkreutz D, Hornung J, Markham A, Fusenig NE (1988) Normal keratinization in a spontaneously immortalized aneuploid human keratinocyte cell line. *J Cell Biol* 106:761–71

Boukamp P, Peter W, Pascheberg U, Altmeier S, Fasching C, Stanbridge EJ *et al.* (1995) Step-wise progression in human skin carcinogenesis *in vitro* involves mutational inactivation of p53, rasH oncogene activation and additional chromosome loss. *Oncogene* 11:961–9

Calautti E, Li J, Saoncella S, Brissette JL, Goetinck PF (2005) Phosphoinositide 3-kinase signaling to Akt promotes keratinocyte differentiation versus death. *J Biol Chem* 280:32856–65

Dajee M, Lazarov M, Zhang JY, Cai T, Green CL, Russell AJ *et al.* (2003) NF-kappaB blockade and oncogenic Ras trigger invasive human epidermal neoplasia. *Nature* 421:639–43

Dijkers PF, Medema RH, Lammers JW, Koenderman L, Coffer PJ (2000) Expression of the pro-apoptotic Bcl-2 family member Bim is regulated by the forkhead transcription factor FKHR-L1. *Curr Biol* 10:1201–4

Greer EL, Brunet A (2005) FOXO transcription factors at the interface between longevity and tumor suppression. *Oncogene* 24:7410–25

Henry MK, Lynch JT, Eapen AK, Quelle FW (2001) DNA damage-induced cell-cycle arrest of hematopoietic cells is overridden by activation of the PI-3 kinase/Akt signaling pathway. *Blood* 98:834–41

Hu MC, Lee DF, Xia W, Golfman LS, Ou-Yang F, Yang JY *et al.* (2004) IkappaB kinase promotes tumorigenesis through inhibition of forkhead FOXO3a. *Cell* 117:225–37

Janes KA, Gaudet S, Albeck JG, Nielsen UB, Lauffenburger DA, Sorger PK (2006) The response of human epithelial cells to TNF involves an inducible autocrine cascade. *Cell* 124:1225–39

Kandel ES, Skeen J, Majewski N, Di Cristofano A, Pandolfi PP, Feliciano CS *et al.* (2002) Activation of Akt/protein kinase B overcomes a G(2)/m cell cycle checkpoint induced by DNA damage. *Mol Cell Biol* 22:7831–41

Kim S, Domon-Dell C, Kang J, Chung DH, Freund JN, Evers BM (2004) Down-regulation of the tumor suppressor PTEN by the tumor necrosis factor-alpha/nuclear factor-kappaB (NF-kappaB)-inducing kinase/NF-kappaB pathway is linked to a default IkappaB-alpha autoregulatory loop. *J Biol Chem* 279:4285–91

Kock A, Schwarz T, Kirnbauer R, Urbanski A, Perry P, Ansel JC *et al.* (1990) Human keratinocytes are a source for tumor necrosis factor alpha: evidence for synthesis and release upon stimulation with endotoxin or ultraviolet light. *J Exp Med* 172:1609–14

Lisby S, Faurschou A, Gniadecki R (2006) The autocrine TNFalpha signalling loop in keratinocytes requires atypical PKC species and NF-kappaB activation but is independent of cholesterol-enriched membrane microdomains. *Biochem Pharmacol* 73(Suppl 4):526–33

Loercher A, Lee TL, Ricker JL, Howard A, Geoghegen J, Chen Z *et al.* (2004) Nuclear factor-kappaB is an important modulator of the altered gene expression profile and malignant phenotype in squamous cell carcinoma. *Cancer Res* 64:6511–23

Medema RH, Kops GJ, Bos JL, Burgering BM (2000) AFX-like Forkhead transcription factors mediate cell-cycle regulation by Ras and PKB through p27kip1. *Nature* 404:782–7

Moore RJ, Owens DM, Stamp G, Arnott C, Burke F, East N *et al.* (1999) Mice deficient in tumor necrosis factor-alpha are resistant to skin carcinogenesis. *Nat Med* 5:828–31

Ozes ON, Mayo LD, Gustin JA, Pfeffer SR, Pfeffer LM, Donner DB (1999) NF-kappaB activation by tumour necrosis factor requires the Akt serine-threonine kinase. *Nature* 401:82–5

Peng XD, Xu PZ, Chen ML, Hahn-Windgassen A, Skeen J, Jacobs J *et al.* (2003) Dwarfism, impaired skin development, skeletal muscle atrophy, delayed bone development, and impeded adipogenesis in mice lacking Akt1 and Akt2. *Genes Dev* 17:1352–65

Ramaswamy S, Nakamura N, Sansal I, Bergeron L, Sellers WR (2002) A novel mechanism of gene regulation and tumor suppression by the transcription factor FKHR. *Cancer Cell* 2:81–91

Ren Q, Kari C, Quadros MR, Burd R, McCue P, Dicker AP *et al.* (2006) Malignant transformation of immortalized HaCaT keratinocytes through deregulated nuclear factor kappaB signaling. *Cancer Res* 66: 5209–15

Schwarz A, Bhardwaj R, Aragane Y, Mahnke K, Riemann H, Metze D *et al.* (1995) Ultraviolet-B-induced apoptosis of keratinocytes: evidence for partial involvement of tumor necrosis factor-alpha in the formation of sunburn cells. *J Invest Dermatol* 104:922–7

Segrelles C, Moral M, Lara MF, Ruiz S, Santos M, Leis H *et al.* (2006) Molecular determinants of Akt-induced keratinocyte transformation. *Oncogene* 25:1174–85

Sun H, Lesche R, Li DM, Liliental J, Zhang H, Gao J *et al.* (1999) PTEN modulates cell cycle progression and cell survival by regulating phosphatidylinositol 3,4,5,-trisphosphate and Akt/protein kinase B signaling pathway. *Proc Natl Acad Sci USA* 96:6199–204

Suzuki A, Itami S, Ohishi M, Hamada K, Inoue T, Komazawa N *et al.* (2003) Keratinocyte-specific Pten deficiency results in epidermal hyperplasia, accelerated hair follicle morphogenesis and tumor formation. *Cancer Res* 63:674–81

Tang TT, Dowbenko D, Jackson A, Toney L, Lewin DA, Dent AL *et al.* (2002) The forkhead transcription factor AFX activates apoptosis by induction of the BCL-6 transcriptional repressor. *J Biol Chem* 277:14255–65

Thorn T, Gniadecki R, Petersen AB, Vicanova J, Wulf HC (2001) Differences in activation of G2/M checkpoint in keratinocytes after genotoxic stress induced by hydrogen peroxide and ultraviolet A radiation. *Free Radic Res* 35:405–16

Tran H, Brunet A, Grenier JM, Datta SR, Fornace AJ Jr, DiStefano PS *et al.* (2002) DNA repair pathway stimulated by the forkhead transcription factor FOXO3a through the Gadd45 protein. *Science* 296: 530–4

Vasudevan KM, Gurumurthy S, Rangnekar VM (2004) Suppression of PTEN expression by NF-kappa B prevents apoptosis. *Mol Cell Biol* 24: 1007–21

Wang HQ, Quan T, He T, Franke TF, Voorhees JJ, Fisher GJ (2003) Epidermal growth factor receptor-dependent, NF-kappaB-independent activation of the phosphatidylinositol 3-kinase/Akt pathway inhibits ultraviolet irradiation-induced caspases-3, -8, and -9 in human keratinocytes. *J Biol Chem* 278:45737–45

Wullschleger S, Loewith R, Hall MN (2006) TOR signaling in growth and metabolism. *Cell* 124:471–84

You H, Yamamoto K, Mak TW (2006) Regulation of transactivation-independent proapoptotic activity of p53 by FOXO3a. *Proc Natl Acad Sci USA* 103:9051–6

Zha J, Harada H, Yang E, Jockel J, Korsmeyer SJ (1996) Serine phosphorylation of death agonist BAD in response to survival factor results in binding to 14-3-3 not BCL-X(L). *Cell* 87:619–28

Zhang JY, Adams AE, Ridky TW, Tao S, Khavari PA (2007) Tumor necrosis factor receptor 1/c-Jun-NH_2-kinase signalling promotes human neoplasia. *Cancer Res* 67:3827–34

Zhang QS, Maddock DA, Chen JP, Heo S, Chiu C, Lai D *et al.* (2001) Cytokine-induced p38 activation feedback regulates the prolonged activation of AKT cell survival pathway initiated by reactive oxygen species in response to UV irradiation in human keratinocytes. *Int J Oncol* 19:1057–61